scientific reports

Check for updates

OPEN

Carbon dot based dressing for therapy of chemically-induced cutaneous burns

Halyna Kuznietsova[1]✉, Arsen Ishchuk[1], Iryna Byelinska[1,3], Tetiana Lysenko[1,4], Volodymyr Melnytsky[1], Olexandr Ogloblya[2], Alexander Zaderko[5], Anna Kalinina[6], Denys Kryvosheiev[1], Vladimir Lysenko[5] & Nataliia Dziubenko[1]

Chemical burns are a significant concern in Ukraine, with a growing interest in new treatments. Carbon-based nanoparticles, due to their anti-inflammatory, antioxidant, and antibacterial properties, have shown promise for wound healing. This study aimed to evaluate the efficacy of carbon dots (CD) derived from citric acid and urea in promoting healing of both acidic- and alkali-induced burns in a rat model. The results indicated that acid-induced burns were slower to heal and exhibited more inflammation compared to alkali-induced burns with the same initial injury level. Daily application of CD dressings significantly reduced the burn area and inflammation in alkali-induced burns during the first week, i.e. accelerated burn healing process, although the treatment was less effective in acid burns. Both types of burns led to increased white blood cell counts, a left shift, and segmented neutrophils by day 7, signaling early acute inflammation. CD dressings notably reduced leukocytosis while preserving neutrophilia and lymphocyte release on days 7 and 14. Furthermore, CD treatment prevented post-burn anemia by maintaining erythrocyte integrity. The immune system's response and inflammation levels were consistent with the burn healing process and skin histopathology. Overall, CD accelerated healing, particularly in alkali burns, and had a systemic effect on immune and inflammatory responses.

Keywords Carbon dots, Acidic-induced burn, Alkali-induced burn, Skin inflammation, Blood cell inflammatory markers

According to the World Health Organization (WHO), burns are a significant global health issue, leading to around 180,000 deaths annually. Burn injuries can have long-lasting effects, even after wounds have healed, impacting both the physical and mental health of patients. Chemical burns, though representing only about 3% of all burn cases (and just over 10% for skin burns specifically), contribute to approximately 30% of burn-related fatalities[1]. They account for 1.4–8.5% of hospital admissions related to burns. Chemical burns can affect the skin, eyes, and internal organs, often leading to systemic damage[2]. These burns typically result from exposure to acidic or alkaline substances. Common acids include fluoric acid, sulfuric acid, and hydrochloric acid, while potassium hydroxide and sodium hydroxide are notable alkaline agents. Acids generally cause tissue damage through protein denaturation and coagulation necrosis, forming thick eschar. Alkaline substances, however, penetrate deeper, causing liquefactive necrosis[3].

Until recently, chemical burns did not hold a significant place among the challenges for Ukraine's healthcare system. However, due to ongoing military actions, trauma-related issues in Ukraine have become exceptionally acute, particularly with a high incidence of burns among the civilian population. One of the most severe forms of burns, in terms of consequences and therapy, is caused by exposure to chemical substances. Furthermore, the mechanisms underlying chemical burns differ fundamentally from those in thermal injuries.

Clinical protocols for treating burn victims and managing the aftermath[4] offer general guidelines, such as pain management, the use of corticosteroids for inflammation, antibiotic therapy, and shock treatment, depending

[1]Institute of High Technologies, Taras Shevchenko National University of Kyiv, Volodymyrska str. 64/13, Kyiv 01601, Ukraine. [2]Physics Department, Taras Shevchenko National University of Kyiv, Kyiv 01033, Ukraine. [3]Educational and scientific center "Institute of Biology and Medicine", Taras Shevchenko National University of Kyiv, Volodymyrska str. 64/13, Kyiv 01601, Ukraine. [4]Palladin Institute of Biochemistry, National Academy of Sciences of Ukraine, 9 Leontovicha Street, Kyiv 01054, Ukraine. [5]Universite Claude Bernard Lyon 1, CNRS, Institut Lumière Matière, UMR5306, Villeurbanne 69100, France. [6]Veterinary clinic Zoolux, Dmytrivska str. 39, Kyiv 02000, Ukraine. ✉email: biophyz@gmail.com

on the injury's severity. However, these protocols lack specific strategies tailored to the unique characteristics of chemical burns. This is primarily due to a limited understanding of the mechanisms behind chemical burn injury and the specific nuances of tissue regeneration that follow. While it is known that thermal and chemical burns differ fundamentally in how they develop and heal, the literature on chemical burns remains scarce. Thus, gaining a clearer understanding of the mechanisms driving chemical burns and the process of tissue regeneration, as well as identifying agents with strong anti-inflammatory, antibacterial, and wound-healing properties, is essential for creating more targeted treatment methods.

Nanoparticles of various kinds, including those based on carbon, have attracted interest for their wide range of effects on biological systems. Carbon nanocomposites, with their embedded heterogeneous atoms and various functional groups, can fluoresce (which is useful for bioimaging)[5], and they possess anti-tumor[6], anti-inflammatory[7], antibacterial, and antiviral properties[8]. These nanoparticles can also either inhibit or stimulate cell growth[9] and are capable of delivering drugs in a targeted manner[10]. Because of these properties, carbon-based nanocomposites show great potential as wound-healing agents, especially in the treatment of burn injuries.

Given this background, the study aimed to explore the capacity of carbon dots, synthesized from citric acid and urea, to enhance the healing of chemically-induced skin burns and to reduce the overall damage caused to the body.

Results

Chemical structure of carbon dots

Figure 1 illustrates the typical schematic chemical structure of the carbon dots (CDs) used in this study. The CDs consist of an sp2-hybridized core, surrounded by surface chemical groups such as carboxyl, phenolic, and amino functional groups. The colloidal solutions of CDs have a yellowish hue but remain transparent when exposed to sunlight. The average size of the synthesized CDs is generally less than 100 nm[5,11–13].

Burn area

For acid-induced burns, a significant reduction in both absolute and relative burn areas was observed in CD-treated animals by days 2–3. Afterward, the healing rate in CD-treated animals followed a similar trend as those treated with Vehicle or left untreated, up until the end of the study (21 days). On the other hand, alkali-induced burns healed more rapidly in CD-treated animals compared to untreated ones. Burn areas, both absolute and relative, were significantly smaller in the CD-treated group on days 1–9 compared to untreated rats (Figs. 2 and 3). Notably, animals treated with Vehicle alone showed burn healing dynamics similar to those of untreated rats, indicating that the incorporation of CD into the Vehicle is essential for effective burn treatment.

Histopathological analysis revealed that rats with acid-induced burns exhibited significant inflammation and edema 7 days post-burn, with tissues heavily populated by inflammatory cells, primarily neutrophils, alongside macrophages and lymphocytes. There were also signs of necrosis and apoptosis. Over the next 14 days, inflammation gradually subsided: by days 14 and 21, apoptosis and necrosis had disappeared, and inflammation and edema were reduced. However, connective tissue accumulation increased, suggesting tissue remodeling and healing. Rats treated with either Vehicle or CD displayed similar patterns, but the signs were less severe than in untreated animals, correlating with the observed burn healing dynamics (Fig. 4).

In the case of alkali-induced burns, a similar histopathological pattern was observed, though the signs of inflammation and tissue damage were less pronounced, and healing occurred more rapidly. By day 7, untreated animals with alkali burns showed inflammation and edema, but with fewer inflammatory cells, especially neutrophils, and no signs of necrosis or apoptosis (Fig. 5), which is in line with the pilot study results[14]. By day 14, the injury site resembled the condition of acid burns on day 21, confirming the faster healing dynamics observed macroscopically (Table 1). So, rats treated with CD exhibited milder signs of injury than untreated or Vehicle-treated animals, consistent with the observed burn healing dynamics (Fig. 2).

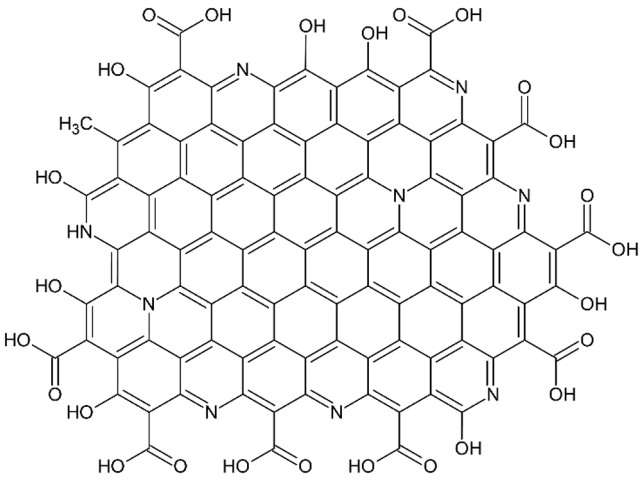

Fig. 1. Typical schematic chemical structure of carbon dots used in this work.

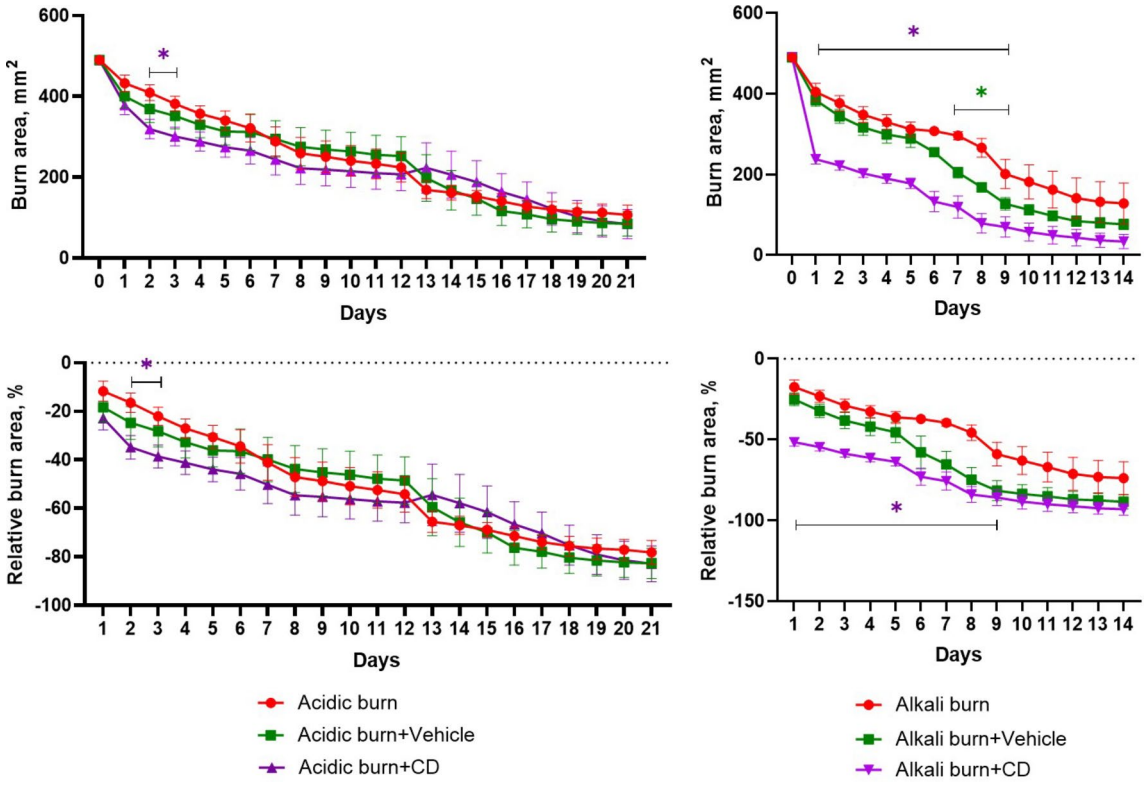

Fig. 2. Burn area dynamics during the study; absolute (top) and relative (bottom) acidic-induced (left panel) and alkali-induced (right panel) burn area changes in animals daily treated with Vehicle or CD-contained dressing; in time interval 0–7 days $n = 12$ and $n = 8$ in acidic- and alkali-induced groups (each treatment group), in time interval 8–14 days $n = 8$ and $n = 4$ in acidic- and alkali-induced groups (each treatment group), in time interval 15–21 days $n = 4$ in acidic-induced groups (each treatment group); $^{*}p < 0.05$ compared to non-treated animals (Burn group), color of the asterisk represents the comparison group on the appropriate day of the study.

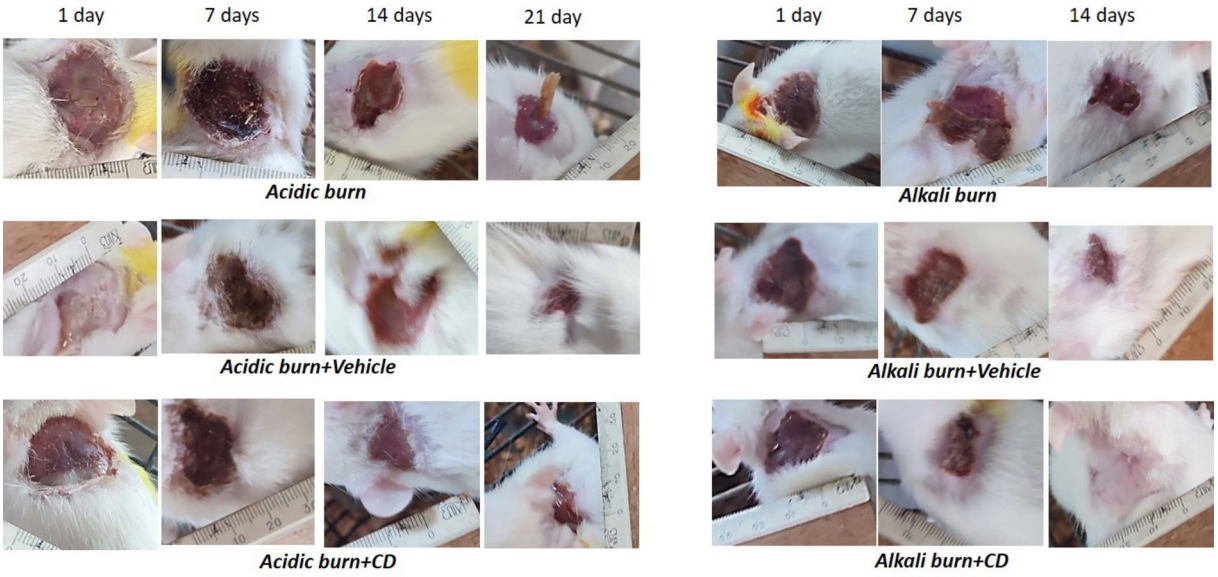

Fig. 3. Photographs of burns of rats experienced acidic- (left panel) and alkali- induced (right panel) cutaneous burns and daily treated with Vehicle or CD-contained dressing at different days of the study.

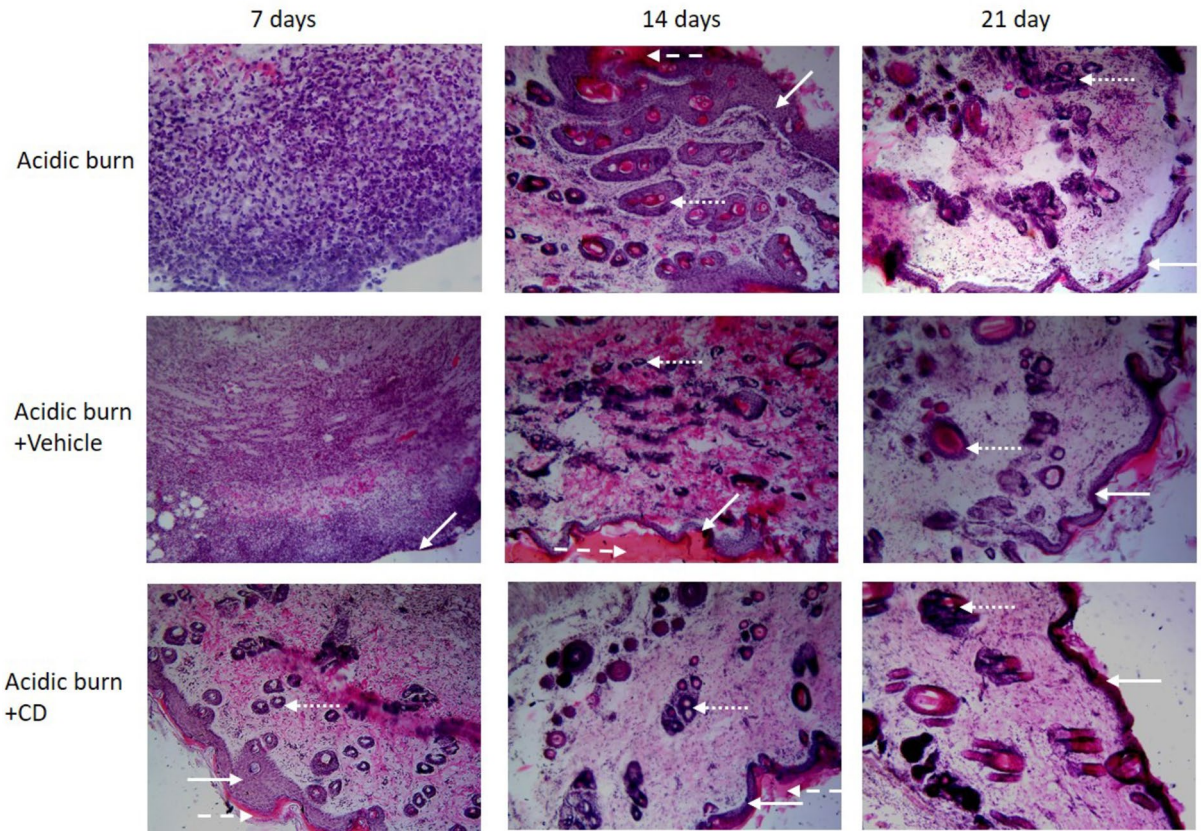

Fig. 4. Representative microphotographs of skin samples from the site of burn of male Wistar rats experienced Acidic-induced burns and treated with Vehicle or CD on different post-burn induction days, H&E staining, Magnification x400. Inflammation, edema, apoptosis and necrosis signs highly expressed at the 7th day with tending down in 14 and 21 days, accompanying with connective tissue accumulation. Solid lines indicate epidermis layer, dotted lines – hair follicles, dashed lines – eschars.

Control samples taken from healthy skin (from the withers) showed a slight presence of macrophages and lymphocytes in the dermis and minimal connective tissue accumulation, which is typical for healthy skin (Fig. 5).

Systemic conditions

Rats from all experimental groups did not lose weight during the study. However, body weight gain slowed down during the entire study compared to healthy animals, and body weights of burn-experienced animals at different time points were significantly lower than that of healthy control (Supplementary Figure S1). Meanwhile, there were also no differences between the burn-experienced groups, regardless of whether they were untreated or treated with either Vehicle or CD.

Analysis of immune-competent organs' weights revealed a trend to decrease of lymph nodes and simultaneous increase of spleen in 14 and 21 days after burn induction in Acidic burn group, which might reflect the changes in immune system (and therefore in immune-associated organs). However, there was no increase in thymus weight in this group (Fig. 6). CD-treated rats exhibited a similar but less pronounced trend, suggesting that CD treatment may have a mitigating effect on the immune response to burns.

In the case of alkali-induced burns, the relative weight of lymph nodes decreased 7 days after burn induction in all burn-experienced groups, whether treated or untreated, which is in line with the data from pilot study[14]. The spleen's weight increased only in the alkali burn groups 14 days after burn induction (Fig. 6). Again, the reactions in CD-treated animals were less pronounced than in untreated or Vehicle-treated animals.

So, similar reactions of immune-competent organs were observed in both Acidic- and Alkali-induced burn models, and the healing effects of CD treatment were comparable to those observed in burn area measurements. Notably, the changes in Alkali-induced groups on 7th and 14th days post-burn induction were similar to those in Acidic-induced groups on 14th and 21st days post-burn induction, respectively. These trends reflect the histopathological changes observed in the affected skin and suggest faster burn healing in alkali-induced burns compared to acid-induced burns, despite the similar initial burn severity.

Analyzing hematological parameters, we observed a significant increase in white blood cell (WBC) count in the acid-induced burn group. The WBC count rose by 32% at day 7 post-burn, remained elevated by 30% through day 14, and returned to baseline by day 21 (Fig. 7). This indicates the development of an inflammatory process, confirmed by a strong correlation between leukocyte count and burn lesion area ($r = 0.864$) and its

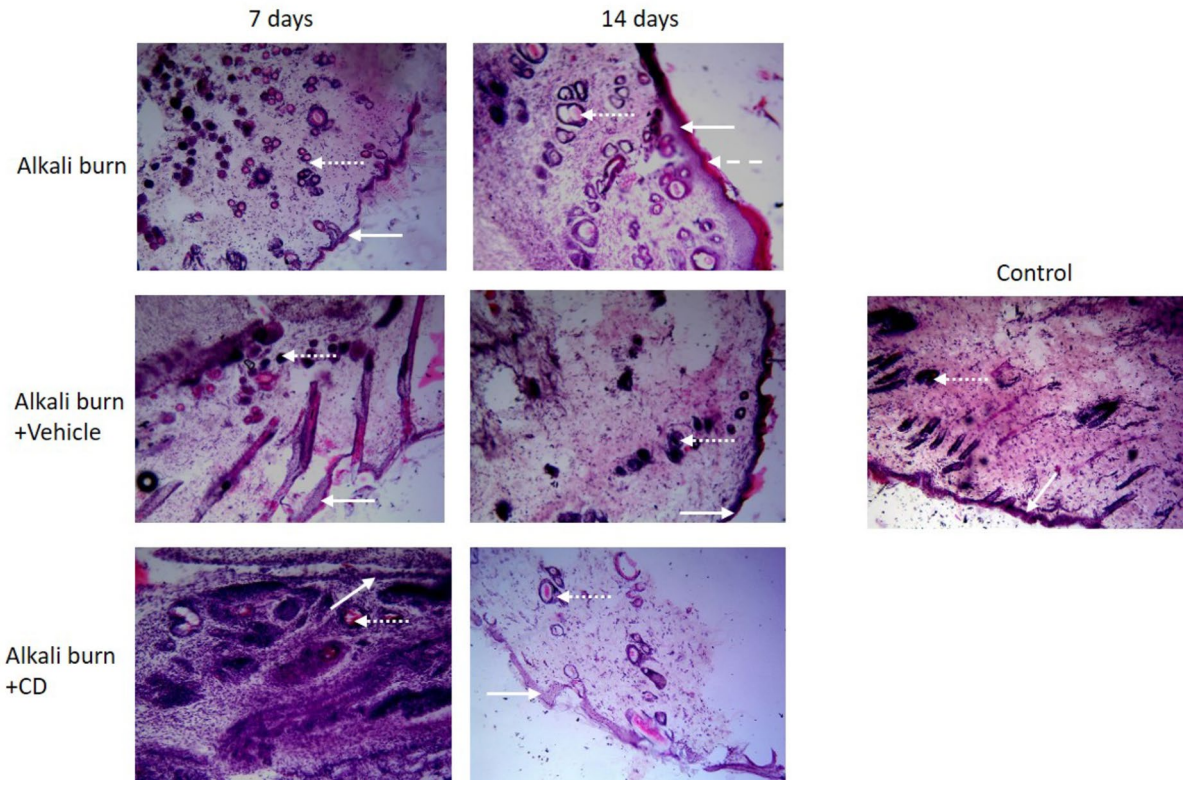

Fig. 5. Representative microphotographs of skin samples from the site of burn of male Wistar rats experienced Alkali-induced burns and treated with Vehicle or CD on different post-burn induction days, H&E staining, Magnification x400. Inflammation and edema expressed at the 7th day with tending down in 14 days, accompanying with connective tissue accumulation. Solid lines indicate epidermis layer, dotted lines – hair follicles, dashed lines – eschars.

Groups	Days	Macrophages	Neutrophils	Lymphocytes	Apoptosis	Necrosis	Edema	Connective tissue	Hemorrhage	Vessel dilation	Total
Control		1 [0;1]	0[0;0]	1[1;1]	0[0;0]	0[0;0]	0[0;0]	1[0;1]	0[0;0]	0[0;1]	3[1;4]
Acidic burn*	7	2[2;3]*	3[2;3]*	2[1;2]	1[1;1]*	1[0;1]	3[3;3]*	0[0;1]	0[0;1]	1[1;1]	13[10;16]
	14	2[2;2]*	2[1;2]*	2[1;2]	0[0;1]	0[0;1]	2[1;2]*	2[1;2]	0[0;0]	0[0;1]	10[6;13]*
	21	1[1;2]	1[1;1]*	1[1;2]	0[0;0]	0[0;0]	1[1;2]*	2[1;2]	0[0;0]	0[0;0]	6[5;9]*
Acidic burn + Vehicle	7	2[1;2]	2[2;2]*	2[1;2]	1[0;1]	1[0;1]	3[2;3]	0[0;0]	0[0;0]	1[1;2]	12[7;13]*
	14	2[1;2]	2[1;2]*	2[1;2]	0[0;1]	0[0;1]	2[2;3]	1[1;2]	0[0;0]	0[0;0]	9[6;13]*
	21	2[0;2]	1[1;2]*	1[1;2]	0[0;0]	0[0;0]	1[1;2]	2[1;2]	0[0;0]	0[0;0]	7[4;10]*
Acidic burn + CD	7	2[1;2]	2[2;3]*	2[1;2]	1[0;1]	1[0;1]	3[2;3]*	0[0;1]	0[0;0]	1[1;2]	12[7;15]*
	14	2[1;2]	1[1;1]*	1[1;1]	0[0;1]	0[0;1]	2[2;2]*	1[1;2]	0[0;0]	0[0;0]	7[6;10]*
	21	2[0;2]	1[1;1]*	1[0;1]	0[0;0]	0[0;0]	1[1;2]*	1[1;2]	0[0;0]	0[0;0]	6[3;6]
Alkali burn	7	2[2;2]*	1[1;1]*	2[1;2]	0[0;0]	0[0;1]	3[2;3]*	1[0;1]	0[0;0]	0[0;1]	9[6;11]*
	14	1[1;2]	1[0;1]	1[1;1]	0[0;0]	0[0;0]	1[1;2]*	2[2;2]*	0[0;0]	0[0;0]	6[5;8]*
Alkali burn + Vehicle	7	2[1;2]	1[1;1]*	2[1;2]	0[0;0]	0[0;1]	2[2;2]*	1[1;1]	0[0;0]	0[0;1]	8[6;10]*
	14	1[1;1]	1[0;1]	1[0;1]	0[0;0]	0[0;0]	1[1;2]*	2[1;2]	0[0;0]	0[0;0]	6[3;7]
Alkali burn + CD	7	2[1;2]	1[0;1]	2[1;2]	0[0;0]	0[0;0]	0[0;1]#	1[1;2]	0[0;0]	0[0;1]	6[3;9]
	14	1[0;1]	0[0;1]	1[1;1]	0[0;0]	0[0;0]	0[0;1]	2[1;2]	0[0;0]	0[0;0]	4[2;6]

Table 1. Sign scores of skin samples (burn site) of male Wistar rats experienced Acidic- and Alkali-induced burns and treated with CD on different days of the study Scores: 0 - <10%; 1–10–50%; 2–50–80%; 3 - >80% of section area occupied; total – sum of the scores; $n = 4$ for each group in each time point. *$p < 0.05$ compared to control (healthy animals), # $p < 0.05$ compared to burn-experienced group in respective time point.

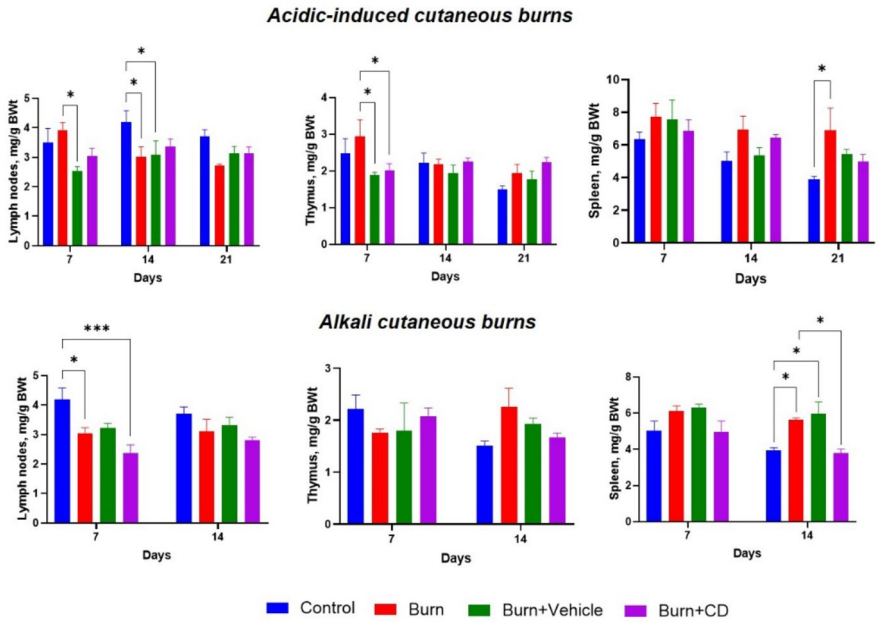

Fig. 6. Relative weights of immune-competent organs of rats experienced burns and treated with Vehicle or CD at the terminal day of the study; $n = 4$ in each group; $^{*}p < 0.05$.

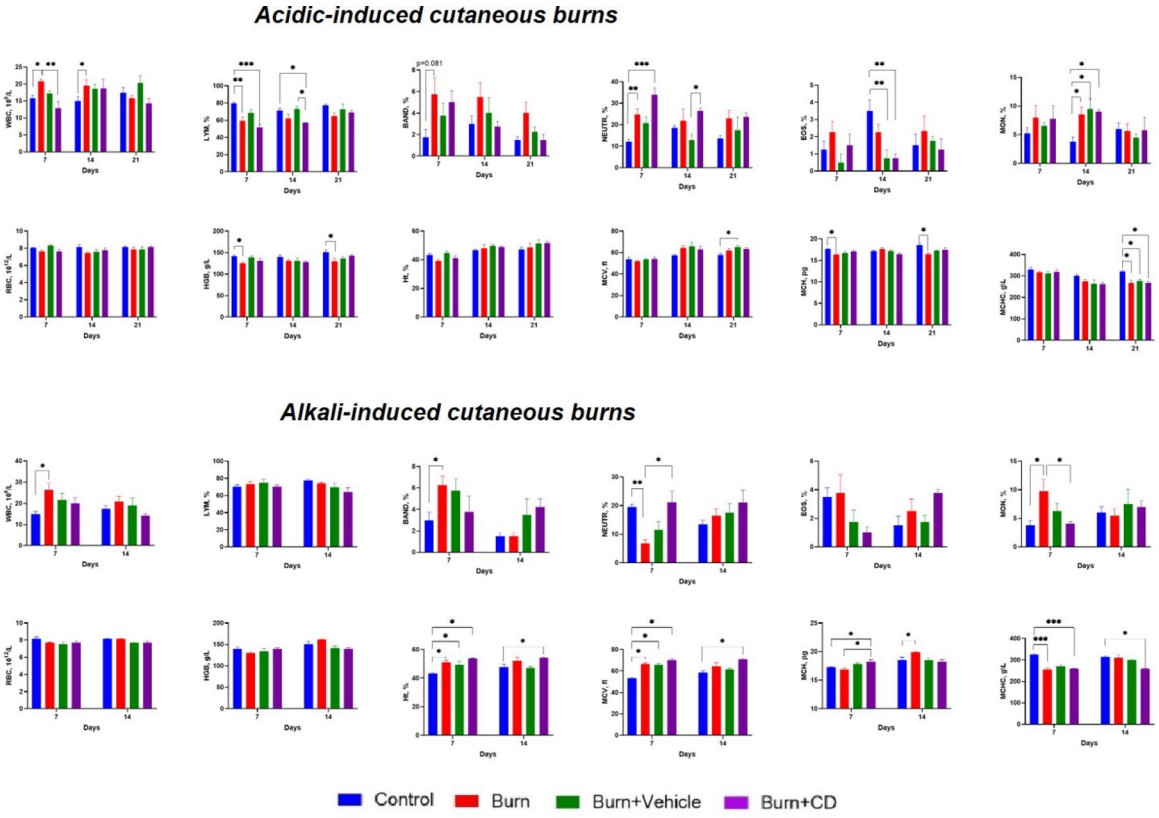

Fig. 7. White blood cell counts and distributions and red blood cells counts and indices of rats experienced burns and treated with Vehicle or CD at the terminal day of the study; where: WBC – WBC absolute count; BAND - band cells, NEUTR – segmented neutrophils, EOS – eosinophilic cells, LYM – lymphocytes, MON – monocytes percentages, RBC – red blood cell count, HGB – hemoglobin, Ht – hematocrit, MCV – mean erythrocyte volume, MCH – mean corpuscular hemoglobin, MCHC – mean corpuscular hemoglobin concentration for acidic-induced (top panel) and alkali-induced (bottom panel) cutaneous burns; $n = 4$ in each group; $^{*}p < 0.05$, $^{**}p < 0.01$, $^{***}p < 0.001$.

resolution over time. We also noted shifts in the distribution of different WBC populations, particularly in the percentages of band cells (BAND%), segmented neutrophils (NEUTR%), and lymphocytes (LYM%). Band cells and segmented neutrophils showed the most significant changes, increasing more than threefold and twofold, respectively, at day 7 post-burn, and gradually returning to control levels by day 21 (Fig. 7). A medium-strength correlation between blood neutrophil percentage and burn area ($r = 0.687$) indicates their active involvement in the inflammatory response. The LYM% decreased significantly at day 7 and showed an inverse correlation with burn area (r=-0.744), reflecting active migration to the injury site and temporary lymphoid impairment. However, LYM% returned to normal levels by day 21 (Fig. 7). These findings are corroborated by our histopathological and gross necropsy observations.

CD treatment effectively inhibited the development of leukocytosis, reducing leukocyte count by 38% compared to the acid burn group on day 7 post-burn, performing better than the vehicle. Despite the reduction in blood leukocyte numbers, CD induced pronounced neutrophilia, increasing it by 2.8 times compared to the control and by 37% compared to the acid-induced burn group ($p = 0.099$), with sustained levels on day 14 post-burn, indicating a potential healing effect of CD. There was a strong correlation ($r = 0.709$) on day 7 and a moderate correlation ($r = 0.512$) on day 14 between blood neutrophil percentage and burn area in case of CD treatment, confirming its stimulatory effect on neutrophilia development. This shift resulted in a 35% reduction in lymphocytes on day 7 and a 19% reduction on day 14. CD also maintained monocyte involvement in the repair process at the same intensity as the vehicle, with significantly elevated monocyte numbers in both treated groups compared to the control on day 14 post-burn (Fig. 7).

Acid-induced burn trauma affected erythrocytes, leading to hypochromic anemia features. Blood hemoglobin concentration and erythrocyte hemoglobin content significantly decreased on days 7 and 21 post-burn without erythrocyte depletion or hematocrit alteration compared to the healthy control. There was also a reduction in erythrocyte hemoglobin concentration on day 21 compared to control. These changes suggest increased erythrocyte turnover, impaired tissue oxygenation, and complications in the burn recovery process. The application of CD dressing, similar to the vehicle, delayed and mitigated erythroid disruption and prevented anemia development, reflecting some healing effects of CD. However, it did not prevent a decrease in hemoglobin concentration, instead increasing erythrocyte volume ($p = 0.073$) on day 21 post-burn (Fig. 7).

In the alkali-induced burn group, we observed a significant increase in WBC count by 75% on day 7 post-burn compared to the healthy control, along with a moderate direct correlation between leukocyte count and burn lesion area ($r = 0.646$), indicating their involvement in the repair process. This is consistent with our findings in the acid-induced burn group. While leukocytosis was evident, it tended to normalize by day 14 post-burn. Notably, on day 7 post-burn, there was more than a twofold increase in band neutrophils, with a moderate direct correlation with burn area ($r = 0.507$). Unlike the acid-induced burn, segmented neutrophil count in the blood was reduced by 65% and had an inverse correlation with burn area (r=-0.687), indicating accelerated migration into the lesion site. Monocytes increased 2.6-fold on day 7 post-burn, earlier than in the acid-induced burn group. Eosinophil and lymphocyte counts were not affected, and all leukocyte disturbances normalized by day 14, suggesting a shorter recovery period compared to the acid burn (Fig. 7), which aligns with our histopathological and observational findings.

CD dressing reduced leukocyte elevation, prevented the increase in band neutrophils, and mitigated the reduction of segmented neutrophils and the development of monocytosis compared to the non-dressed alkali-induced burn group, bringing levels closer to control on day 7 post-burn. This suggests that CD was more effective than the vehicle in mitigating burn-induced inflammation and promoting skin injury resolution, consistent with our histopathological findings (Fig. 7).

Similar to the acid-induced burn model, the alkali-induced burn demonstrated a mild modulating effect on blood erythrocytes. There was a slight increase in hematocrit and MCV, with a subsequent reduction in MCHC, likely due to erythrocyte swelling from tissue-destructive and inflammatory molecules. The application of CD maintained these erythrocyte modulation effects and even slightly stimulated erythrocyte development (Fig. 7). These changes are not clinically significant and do not complicate the burn resolution process, but they could be noteworthy in cases of more severe burns or in studies of CD interactions with erythrocytes.

To summarize, blood leukocytes—particularly band and segmented neutrophils and monocytes for both acidic- and alkali-induced cutaneous burns, and lymphocytes for acidic-induced burns—can be considered indicative parameters of the healing effect of CD post-burn and can be easily monitored. Additionally, monitoring erythrocyte indices is recommended to prevent anemia, which can complicate the burn healing process.

Fluctuations in IL-6 and IL-10 levels at different time points in both models were not significant, preventing any conclusions about strong systemic inflammation (Supplementary Figure S2).

Biochemical analysis revealed fluctuations in liver functional enzyme activity in the serum of all groups (both acidic- and alkali-induced models). However, even statistically significant changes were not dramatic and did not indicate liver toxicity or any specific trends in liver function during the burn healing process (Supplementary Figures S3, S4). Additionally, creatinine and urea levels remained unchanged across all experimental groups (Supplementary Figure S5), suggesting no impact on kidney function during burn injury resolution.

Discussion

CDs have emerged as promising agents in managing both acute and chronic wounds, including burns, due to their multifunctional properties such as antibacterial effects, anti-inflammatory actions, and regenerative potential. Their unique physicochemical properties, excellent biocompatibility, and capacity to modulate wound-healing processes make them ideal candidates for advancing therapeutic strategies[15]. Recent studies indicate that CDs can significantly enhance wound healing by addressing key challenges such as oxidative stress and bacterial infections, which are critical barriers in wound recovery. In particular, CDs have been shown to enhance wound healing by modulating reactive oxygen species (ROS) levels. The surface of the CDs used in our study

is enriched with carboxyl and phenolic groups, enabling them to effectively scavenge free radicals and exhibit strong antioxidant properties. It is well-established that the presence of phenolic groups significantly enhances a molecule's antioxidant capacity – the greater the number of phenolic groups, the stronger its antioxidant potential[16]. Based on this, we propose that our CDs possess robust antioxidant properties. Controlled ROS production is crucial for various stages of wound healing, including inflammation, proliferation, and tissue remodeling. Small concentrations of ROS are necessary to combat invading bacteria and guide cells to the wound site, facilitating the repair process[17]. However, excessive and uncontrolled oxidative stress can lead to chronic inflammation, contributing to the pathogenesis of non-healing wounds. Maintaining a sensitive balance between the beneficial and harmful effects of ROS is essential for effective ulcer treatments and proper wound healing[18]. The same is applicable to cutaneous burns: oxidative stress markers, such as malondialdehyde (MDA), increase significantly after chemical burns. Additionally, antioxidant defenses, including reduced glutathione levels, catalase, superoxide dismutase, glutathione S-transferase, glutathione peroxidase, and glutathione reductase, are depleted in the long term after chemical exposure[19]. Strategies targeting oxidative stress, such as antioxidant therapies and photobiomodulation, may be beneficial in promoting burn wound healing. To reduce ROS levels in wounds, several ROS-scavenging materials have been incorporated into hydrogel dressings, such as antioxidants, enzymes, and nanomaterials[20]. These hydrogels, which can be sprayable or injectable, offer sustained release and antioxidant properties that provide potential benefits for wound healing[21].

The primary driver of ROS production is neutrophils, the first line of innate immunity that arrives at the injury site during the first post-injury week, as demonstrated in previous studies on colon chemical burns and skin thermal burns[22,23]. The active migration of neutrophils through the blood, associated with neutrophilia, indicates an acute inflammatory response[24]. In our study, we showed that both acidic and alkaline skin burns induce an acute inflammatory process, evidenced by increased band (left shift) and segmented neutrophils in the blood. This experimental evidence confirms that these cells are early markers of chemical burns. Their accumulation and activation at the lesion site result in ROS production, which expands the damaged tissue area, necessitating control to reduce the affected area. The effectiveness of such approaches has been demonstrated in chemical colon burns, resulting in reduced colitis severity[24], and other conditions accompanied with excessive ROS production[25]. We demonstrated that CD dressing of the burn site stimulates neutrophil migration through the bloodstream and, combined with CD's ability to scavenge ROS due to its chemical structure, promotes and enhances the skin repair process. CD also have been shown to regulate the infiltration of neutrophils and lymphocytes to the wound site, minimizing tissue damage while maintaining sufficient immune surveillance[22,26]. Our findings in inflammatory cell population of burn site and their changes throughout the course of burn resolution are in line with this statement.

It's not just neutrophils involved in the pathological process and ROS production. In the first week post-alkaline cutaneous burn, there is an elevated monocyte count in the blood and macrophage accumulation at the lesion site. In contrast, acidic-induced cutaneous burns elevate blood monocytes later, towards the end of the second week post-burn, likely due to coagulation induction rather than alkali-induced liquefactive necrosis. ROS neutralization using scavengers could accelerate the healing process[23,27], aiming to reduce hospitalization periods and work capacity limitations, and might be further used for elaborating treatment protocols.

CDs can effectively neutralize lipopolysaccharide-triggered ROS production by macrophages, promoting their polarization from a pro-inflammatory (M1) towards an anti-inflammatory (M2) phenotype. This switch is essential for the resolution of inflammation and the promotion of burn healing[28–30]. Reduction of excessive inflammation at the wound site by CDs might happen by modulating immune responses and reducing pro-inflammatory cytokines. Although we did not observe statistically significant differences in IL-6 (a pro-inflammatory cytokine) or IL-10 (an anti-inflammatory cytokine) levels, the involvement of cytokines in the anti-inflammatory action of CDs cannot be entirely excluded. However, it appears that cytokine modulation is not the primary mechanism in this specific case. Moreover, given that other cytokines, such as IL-1 and TGF-β, are known to play critical roles in burn healing[18,26], it is plausible that these factors may mediate the healing effects of CDs. Our preliminary results allow us to suggest that CDs inhibit M1 polarization while maintaining M2 polarization. While favoring the M2 phenotype, which is associated with tissue repair and regeneration, CD can also stimulate collagen production, matrix deposition and tissue remodeling[30], which we also observed in our study in burn sites. This study showed that CD reduced blood monocyte count in the first week post-burn, likely affecting M1 precursors, but maintained elevated counts by the second post-burn week, affecting M2 precursors. Thus, CDs help minimize chronic inflammation and promote a more balanced healing process[22,26].

In vitro scratch assays have shown that CDs stimulate epithelial cell migration, which is a vital process in wound healing. They influence cellular signaling pathways that promote the movement of cells to the wound site. This results in faster vascular healing and improved wound recovery, as evidenced by more complete epithelial layer formation, thicker epidermal recovery, and well-organized collagen fibers[26]. This is particularly important during the inflammatory and proliferative phases of wound healing, where cell migration helps in clearing debris and forming new tissue[31]. Then, it was confirmed that topical application of CDs significantly improves wound healing through enhanced fibroblast proliferation, angiogenesis, and collagen deposition[23], which is in line with our findings. This leads to improved collagen synthesis and new blood vessel formation, critical for healing wounds and other injuries, including burns.

CDs also exhibit significant antibacterial actions through multiple mechanisms[32]. This helps to prevent bacterial infections, which hinder wound and burn healing. Then, certain features of erythrocyte preservation help prevent the development of post-chemical burn anemia, which often complicates inflammation and regenerative processes following thermal burns[24,27].

There might be appeared a question about CDs penetrating through epithelial barrier while applied topically. The penetration of nanomaterials, including carbon-based nanoparticles, through intact skin following topical application remains a subject of debate[33]. However, there is a consensus among researchers regarding the ability

of nanoparticles to penetrate damaged skin. The recent study focuses on the application of CDs on compromised skin, making their penetration through the disrupted barrier highly plausible. Consequently, the systemic effects of CDs could arise either from direct penetration through the damaged epithelial barrier or indirectly through their impact on the burn healing process. Significant toxicity of CDs is highly unlikely in this context due to the small applied dose, even when absorbed through damaged skin. Furthermore, our previous studies have demonstrated that the tested CDs exhibit no substantial systemic toxicity, even after repeated parenteral administrations at much higher doses[11].

Summarizing, acid-induced burns took longer to heal and were more inflamed compared to alkali-induced burns with the same initial level of injury. CD everyday dressing significantly decreased the burn area and the level of inflammation in burn site during the first week of burn healing in case of Alkali-induced burn, but much poorer in case of Acidic-induced one. The suggested mechanisms of this action may involve anti-inflammatory action (confirmed by hematological data and histopathological findings in burn site), and ability to modulate immune response in burn site by influencing the macrophage M1-to-M2 polarization and enhancing tissue remodeling (confirmed by histopathological findings in burn site). There were almost no substantial systemic toxicity of burn (of such area) and its healing. Immune system reaction persisted during the entire burn healing process, and the effects of CD treatment on that were in line with the dynamics of burn healing and burn histopathology, confirming their immune-modulatory effects. It should be noted, that CDs demonstrated promising potential across various applications, particularly within environmental and biomedical domains. Their unique attributes, such as excellent biocompatibility and customizable photochemical properties, position them as versatile candidates for numerous functional roles. However, despite significant progress, challenges persist in achieving rational design and consistent application of CDs, especially in regulatory contexts. Addressing these issues through further research is crucial to optimize their properties for practical implementation[34].

Overall, the application of carbon dots in wound healing shows promising results by accelerating tissue regeneration, enhancing cell migration, and modulating inflammatory responses. These properties make CDs a valuable tool in developing advanced burn care treatments and therapeutic strategies for tissue repair.

Materials and methods

Carbon dots (CDs) synthesis

The carbon dots (CDs) used in this study were synthesized through solvothermal carbonization of a mixture of urea and anhydrous citric acid in a molar ratio of 2:1, with a total mixture mass of 10 g. The components were first ground together in a mortar and then transferred to a 100-ml Pyrex glass reactor. This open reactor was placed in a shaft furnace, where the temperature was gradually increased to 135 °C over 15 min. The mixture was held at this temperature for one hour, during which it melted and took on a yellow hue. Subsequently, the temperature was raised to 165 °C over a 10-minute period and maintained for another hour. During this phase, water, carbon dioxide, and ammonia were visibly released. As the carbonization process neared completion, gas or vapor emissions largely ceased, and the melt solidified into a brown-black, glossy, brittle substance. This carbonized material was dissolved in 80 ml of 15% aqueous isopropanol with gentle heating and then acidified with 10 ml of glacial acetic acid, causing the carbon nanoparticles to coagulate and form a precipitate. The precipitate was filtered and dried at 120 °C in air. Additional details regarding the synthesis and characterization of the CDs can be found in our previous publications[5,11–13].

Topical dressing preparation

To prepare the CD dressing, a solution of CDs in saline (1 mg/mL) was mixed with Hydrosorb Gel, a commercially available hydrogel made up of Ringer's solution, carboxyethyl cellulose, and carboxymethyl cellulose, at a 1:1 ratio. Cellulose-based hydrogels, commonly used for wound and burn treatments, were chosen to serve as both the carrier for the CDs and as a comparison in this study.

Animals

The study was conducted on young male Wistar rats with initial body weight ranged from 152.7 to 197.5 g (CV = 12.8%). Animals were bred in-house and kept in the animal facility of the Taras Shevchenko National University of Kyiv under natural lightning at 20–23 °C, and free access to standardized rodent diet and tap water. All experiments were conducted in compliance with bioethics principles, legislative norms and provisions of the European Convention for the Protection of Vertebrate Animals used for Experimental and Other Scientific Purposes, ARRIVE guidelines, General Ethical Principles for Experiments on Animals, adopted by the First National Bioethics Congress (Kyiv, 2001). All in vivo protocols were approved by Institutional Animal Care and Use Committee of Taras Shevchenko National University of Kyiv (Protocol 3, dated 2.05.2019).

Burn induction and group division

Animals were randomized to the groups based on their body weight the day prior to the burn induction (day − 1). For the simulation of chemically-induced burns, rats were anesthetized using telazol (5 mg/kg, administered intraperitoneally) and xylazine hydrochloride (8 mg/kg, given intramuscularly), and the fur on their upper back was shaved. Gauze discs with a diameter of 2.5 cm (approximately 490 mm^2) were soaked in either 3 N NaOH or 10 N HCl solutions and applied to the skin for 10 min [with modification]. Such conditions lead to second-degree burns induction, as deep dermis damage occurred[35–37], which was also confirmed by our pilot study[14]. This level of burn was selected because it represents the most common depth of skin injury in humans[2]. One hour after burn induction, a dressing containing either the vehicle or carbon dots (CDs) was applied to the burn area, with treatments repeated daily.

For acidic-induced burns, there were 4 groups of male Wistar rats, $n = 12$ in each group: (1) group 1 (Control) – healthy rats with no burns; (2) group 2 (Acidic burn) – rats subjected to acidic burn induction and received no

treatment; (3) group 3 (Acidic burn + Vehicle) - rats subjected to acidic burn induction, Hydrosorb gel (served as a vehicle) was applied on the burn in 1 h after induction and thereafter daily for 20 days; (4) group 4 (Acidic burn + CD) - rats subjected to acidic burn induction, CD-contained dressing was applied on the burn in 1 h after induction and thereafter daily for 20 days. Necropsies with blood and skin samples collection and fixation were performed at the terminal sacrifice on the 7th, 14th and 21st days, where 4 rats from each group were assigned randomly.

For alkali-induced burns, there were 4 groups of male Wistar rats, $n = 8$ in each group: 5) group 5 (Control) – healthy rats with no burns; 6) group 6 (Alkali burn) – rats subjected to alkali burn induction and received no treatment; 7) group 7 (Alkali burn + Vehicle) - rats subjected to alkali burn induction, Hydrosorb gel was applied on the burn in 1 h after induction and thereafter daily for 13 days; 8) group 8 (Alkali burn + CD) - rats subjected to alkali burn induction, CD-contained dressing was applied on the burn in 1 h after induction and thereafter daily for 13 days. Necropsies with blood and skin samples collection and fixation were performed at the terminal sacrifice on the 7th and 14th days, where 4 rats from each group were assigned randomly. Euthanasia was performed under CO_2 anesthesia followed by cervical dislocation.

After every necropsy blood and skin samples from the burn area were collected, and immune-competent organs were weighed.

Burn area measurements

To track the progress of burn healing, photographs of the burns were taken daily before dressing application. The area of the burns was measured from these photographs using ImageJ 1.8.0_172 software (NIH, USA, https://imagej.net/software/fiji/). Each day, the change in burn area was calculated as a percentage change from the initial burn area (defined as the area of the NaOH/HCl-soaked disc application) for each individual animal. The exact area of the burns on Day 0 was not recorded, as the full extent of the burn became apparent only on Day 1. This initial difference in the burn area may reflect varying responses of treated and untreated skin in the first 24 h post-burn.

Biochemical and hematological analyses

For biochemical analysis, blood samples were collected immediately after anesthesia from the femoral vein, and serum was separated after centrifugation. Biochemical markers including alanine aminotransferase (ALT), aspartate aminotransferase (AST), g-glutamyl transpeptidase (GGT), lactate dehydrogenase (LDH), alkaline phosphatase (ALP), urea, and creatinine were analyzed in the serum using commercial kits from DiagnosticumZrt, Hungary, following the manufacturer's instructions.

Blood cell indices including red blood cell count, blood haemoglobin concentration, hematocrit, mean corpuscular volume (MCV), mean corpuscular haemoglobin (MCH), mean corpuscular haemoglobin concentration (MCHC), and white blood cell count were evaluated using conventional methods[38]. Briefly, the hemoglobin concentration was measured using colorimeter (KFK-3, Ukraine) and Hemoglobin Assay Kit (Felicit-Diagnostics, Ukraine). The red blood cells, white blood cells and platelet were counted using a hemocytometer and light microscope (MICROmed XS-3320, Ningbo Shenghens Optics & Electronics). The hematocrit was measured after centrifugation of blood into micro hematocrit capillary. MCH, MCHC and MCV were calculated according to formula.

The leukograms were analyzed differentially using blood smears stained with Pappenheim. A total of 100 white blood cells, including eosinophilic, basophilic, and neutrophilic granulocytes, lymphocytes, and monocytes, were counted. Analysis was performed by experienced pathologist who was unaware of the treatment groups.

ILs analyses

IL-6 and IL-10 were determined in blood serum using commercial kits (Merck, USA).

Histopathological analyses

In order to conduct histopathological analysis, skin specimens were extracted from the burn site of each animal immediately upon collection and immersed in a solution of 10% neutral buffered formalin. These samples underwent processing for hematoxylin and eosin (H&E) staining[39] and were then examined under a light microscope. The analysis focused on assessing the presence and predominance of immune response cells (macrophages, neutrophils, lymphocytes), as well as evaluating features including edema, apoptosis, necrosis, hemorrhages, and accumulation of connective tissue. Analysis was performed by experienced pathologist who was unaware of the treatment groups.

Statistical analysis

Statistical analysis of the data was performed using either two-way (burn area dynamics) or one-way ANOVA (using GraphPad Prism v.10.0.0 software, https://www.graphpad.com/), correlation analysis between white blood cell indices and burn area was performed using the same software. Histopathological scores were compare using U-test for non-parametric data. The parametric data was presented as Mean ± SEM, non-parametric data was presented as media [1st ; 3rd quartiles]; the difference was considered statistically significant at $p < 0.05$.

Data availability

All data generated and analyzed during the in vivo studies are included in this paper and its supplementary information. The datasets corresponding to the characterization of the CD are available from the corresponding author on reasonable request.

Received: 22 September 2024; Accepted: 17 February 2025
Published online: 31 March 2025

References

1. Hardwicke, J., Hunter, T., Staruch, R. & Moiemen, N. Chemical burns - an historical comparison and review of the literature. *Burns* **38**, 383–387 (2012).
2. Koh, D. H., Lee, S. G. & Kim, H. C. Incidence and characteristics of chemical burns. *Burns* **43**, 654–664 (2017).
3. Abbasi, H., Dehghani, A., Mohammadi, A. A., Ghadimi, T. & Keshavarzi, A. The epidemiology of chemical burns among the patients referred to burn centers in Shiraz, Southern Iran, 2008–2018. *Bull. Emerg. Trauma.* **9**, 195–200 (2021).
4. Ministry of Health of Ukraine. Standard of burns medical care, Order No. 1767 dated 09.10.2023. Retrieved from [https://moz.gov.ua/article/ministry-mandates/nakaz-moz-ukrainivid-06102023--1767-pro-zatverdzhennja-standartu-medichnoi-dopomogi-opiki](in Ukrainian).
5. Mussabek, G. et al. Photo- and radiofrequency-induced heating of photoluminescent colloidal carbon dots. *Nanomaterials* **12**, 2426 (2022).
6. Yu, Z. et al. A new approach to upgrade cancer diagnosis and treatment. *Nanoscale Res. Lett.* **16**, 88 (2021).
7. Lee, B. C. et al. Graphene quantum dots as anti-inflammatory therapy for colitis. *Sci. Adv.* **6**, e2630 (2020).
8. Ghirardello, M., Ramos-Soriano, J. & Galan, M. C. Carbon dots as an emergent class of antimicrobial agents. *Nanomaterials (Basel).* **11**, 1877 (2021).
9. Lu, F. et al. Hydroxyl functionalized carbon dots with strong radical scavenging ability promote cell proliferation. *Mater. Res. Express.* **6**, 065030 (2019).
10. Park, J. & Kim, Y. C. Topical delivery of 5-fluorouracil-loaded carboxymethyl chitosan nanoparticles using microneedles for keloid treatment. *Drug Deliv Transl Res.* **11**, 205–213 (2021).
11. Kuznietsova, H. et al. In vitro and in vivo toxicity of carbon dots with different chemical compositions. *Discover Nano.* **18**, 111 (2023).
12. Ivanov, I. I. et al. Photoluminescent recognition of strong alcoholic beverages with carbon nanoparticles. *ACS Omega.* **6**, 18802–18810 (2021).
13. Dubyk, K. et al. Bio-distribution of carbon nanoparticles studied by photoacoustic measurements. *Nanoscale Res. Lett.* **17**, 127 (2022).
14. Kuznietsova, H. et al. Carbon dot dressing as a treatment of alkali-induced skin burns. *Stud. Biologica* **18**, 12–30 (2023).
15. Pooja, S. et al. Carbon-based nanostructured materials for effective strategy in wound management. *Nanostructured Mater. Effective Strategy Wound Manage.* https://doi.org/10.1016/b978-0-323-99165-0.00013-7 (2024).
16. Biela, M., Kleinová, A. & Klein, E. Phenolic acids and their carboxylate anions: thermodynamics of primary antioxidant action. *Phytochemistry* **200**, 113254 (2022).
17. Varmazyar, M., Kianmehr, Z., Faghihzadeh, S. & Ghazanfari, T. Time course study of oxidative stress in sulfur mustard analog 2 chloroethyl ethyl sulfide-induced toxicity. *Int. Immunopharmacol.* **73**, 81–93 (2019).
18. Cheng, H. et al. Sprayable hydrogel dressing accelerates wound healing with combined reactive oxygen species-scavenging and antibacterial abilities. *Acta Biomater.* **124**, 219–232 (2021).
19. Ren, Y. et al. Injectable and antioxidative HT/QGA hydrogel for potential application in wound healing. *Gels* **7**, 204 (2021).
20. Byelinska, I. V. et al. Anti-inflammatory and anti-anemic properties of nanocomplex based on C60 fullerenes and pyrrole core under acute ulcerative colitis in rats. *IEEE Int. Conf. Nanomaterials: Appl. Prop.* **11**, 1–6 (2021).
21. Laggner, M. et al. Severity of thermal burn injury is associated with systemic neutrophil activation. *Sci. Rep.* **12**, 1654 (2022).
22. Byelinska, I. V. et al. Effect of C60 fullerenes on the intensity of colon damage and hematological signs of ulcerative colitis in rats. *Mater. Sci. Eng. C Mater. Biol. Appl.* **93**, 505–517 (2018).
23. Cheng, H. et al. The potential of novel synthesized carbon dots derived from resveratrol using a one-pot green method in accelerating in vivo wound healing. *Int. J. Nanomed.* **18**, 6813–6828 (2023).
24. Weiss, G., Ganz, T. & Goodnough, L. T. Anemia of inflammation. *Blood* **133**, 40–50 (2019).
25. Geng, H. et al. Carbon dot nanozymes as free radicals scavengers for the management of hepatic ischemia-reperfusion injury by regulating the liver inflammatory network and inhibiting apoptosis. *J. Nanobiotechnol.* **21**, 500. https://doi.org/10.1186/s12951-023-02234-1 (2023).
26. Tang, T. et al. Carbon quantum dots as a nitric oxide donor can promote wound healing of deep partial-thickness burns in rats. *Eur. J. Pharm. Sci.* **183**, 106394 (2023).
27. Tichil, I., Rosenblum, S., Paul, E. & Cleland, H. Treatment of anaemia in patients with acute burn injury: a study of blood transfusion practices. *J. Clin. Med.* **10**, 476 (2021).
28. Schilrreff, P. & Alexiev, U. Chronic inflammation in non-healing skin wounds and promising natural bioactive compounds treatment. *Int. J. Mol. Sci.* **23**, 4928 (2022).
29. Gujju, R. et al. Carbon dots' potential in wound healing: inducing M2 macrophage polarization and demonstrating antibacterial properties for accelerated recovery. *ACS Appl. Bio Mater.* **6**, 4814–4827 (2023).
30. Davoodvandi, A. et al. Medicinal plants as natural polarizers of macrophages: phytochemicals and pharmacological effects. *Curr. Pharm. Des.* **25**, 3225–3238 (2019).
31. Azam, M. et al. Curcumin preconditioning enhances the efficacy of adipose-derived mesenchymal stem cells to accelerate healing of burn wounds. *Burns Trauma.* **9**, tkab021. https://doi.org/10.1093/burnst/tkab (2021).
32. Lysenko, V. et al. Application of carbon dots as antibacterial agents: a mini review. *BioNanoSci* **14**, 1819–1831 (2024).
33. Schneider, M., Stracke, F., Hansen, S. & Schaefer, U. F. Nanoparticles and their interactions with the dermal barrier. *Dermatoendocrinol* **1** (4), 197–206. https://doi.org/10.4161/derm.1.4.9501 (2009).
34. Xiuxun, H. et al. Aiguo, W. Carbon Dots in the pathological microenvironment: ROS Producers or scavengers? *Adv. Healthc. Mater.* https://doi.org/10.1002/adhm.202402108 (2024).
35. Goertz, O. et al. Intravital pathophysiological comparison of acid- and alkali-burn injuries in a murine model. *J. Surg. Res.* **182** (2), 347–352 (2013).
36. Grosu, O. M. et al. Experimentally induced burns in rats treated with innovative polymeric films type therapies. *Biomedicines* **11**, 852 (2023).
37. Guo, H. F., Ali, R. M., Hamid, R. A., Zaini, A. A. & Khaza'ai, H. A new model for studying deep partial-thickness burns in rats. *Int. J. Burns Trauma.* **7** (6), 107–114 (2017).
38. Alemu, Y., Atomsa, A. & Sahlemariam, Z. *Hematology* 549EPHTI, (2006).
39. Kiernan, J. A. *Histological and Histochemical Methods: Theory and Practice* (Scion, 2008).

Author contributions

Conceptualization, [HK, VL, ND]; methodology, [HK, ND]; validation, [HK, ND]; formal analysis, [HK, VL, ND].; investigation, [HK, ND, AI, IB, AK, DK, VM, TL, OO, AZ]; resources, [HK, ND, VL]; data curation, [ND, TL, IB]; writing – original draft preparation, [HK, IB]; writing – review and editing, [HK, VL, ND, IB]; visualization, [HK, IB] supervision, [ND]; project administration, [ND]; funding acquisition, [HK, ND, VL]. All authors have read and agreed to the published version of the manuscript.

Funding
This research was funded by EU Horizon 2020 Research and Innovation Staff Exchange Programme (RISE) under Marie Skłodowska-Curie Action (project 101008159 "UNAT"), and Ministry of Education and Science of Ukraine (Grant #23BP07-02). A. Zaderko was also supported by French Government in frame of PAUSE programme.

Declarations

Conflict of interest
The authors declare that the research was conducted in the absence of any commercial or financial relationships that could be construed as a potential conflict of interest.

Human rights
This article does not contain any studies with human subjects performed by the any of the authors.

Animal studies
All institutional, national, and institutional guidelines for the care and use of laboratory animals were followed.

Additional information
Supplementary Information The online version contains supplementary material available at https://doi.org/10.1038/s41598-025-90893-5.

Correspondence and requests for materials should be addressed to H.K.

Reprints and permissions information is available at www.nature.com/reprints.

Publisher's note Springer Nature remains neutral with regard to jurisdictional claims in published maps and institutional affiliations.